Laterally Coupled Quartz Resonators

Steffen Berg and Diethelm Johannsmann*

Max-Planck-Institute for Polymer Research, Ackermannweg 10, 55128 Mainz, Germany

By placing two pairs of electrodes onto a single plate of an AT-cut quartz crystal, one can obtain a device with two separate resonating units on one and the same quartz blank. Energy trapping confines the area of oscillation to a region around the individual electrodes. If the two resonators are spaced close enough to each other, the oscillating regions slightly overlap and coupling occurs. The coupling can be modeled with an equivalent circuit based on two Butterworth−van Dyke circuits connected across a complex resistance providing the coupling. For sufficiently decoupled oscillators, one electrode pair can serve as a reference resonator for microbalance applications. The reference resonator experiences the same environment as the sensing resonator and can therefore be used to measure and subtract effects of temperature, viscosity, and hydrostatic pressure of the ambient medium.

Quartz crystal resonators are widely used to monitor the physical properties of thin layers deposited on their surfaces.[1−3] For example, a specific adsorption of an analyte to a suitably coated quartz surface may be probed via the shift of the resonance frequency.[4] The resonances of thickness shear resonators are extremely sharp, allowing for a very accurate determination of deposited mass. The sensitivity is well into the monolayer regime. However, the accuracy is often limited by environmental factors such as temperature, viscosity, or hydrostatic pressure of the ambient medium. Depending on the details of the experiment, these disturbances can easily be as large as the effect of interest, which could, for instance, be a frequency shift caused by adsorption of an analyte. Keeping the environmental conditions constant is sometimes difficult or even impossible. While the temperature in a flow cell can be maintained constant with some effort, the viscosity necessarily varies with the concentration of the analyte (or other components of the fluid). To distinguish these disturbances from the effect of deposited mass, a reference resonator exposed to the same environment as the sensing resonator is often employed. The same concept can be used to discriminate between specific adsorption to a surface functionalized with certain receptors and unspecific adsorption to a reference surface lacking these recognition sites.

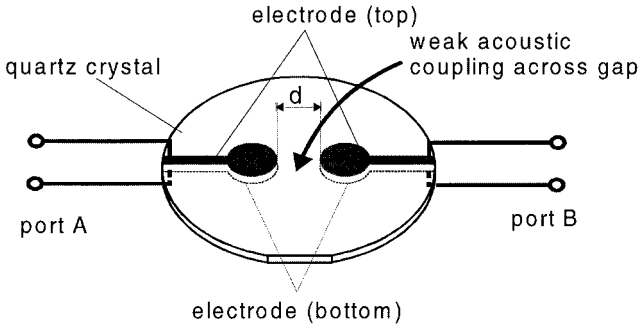

Figure 1. Quartz crystal with two electrode pairs.

We propose the use of two electrode pairs on one and the same quartz plate, providing a sensing and a reference resonator in close proximity. When the two resonators have different surface functionalities, differential measurements of adsorption are straightforward. In the simplest case, the two resonators are spaced so widely apart that they are decoupled. One can then detect the resonance properties of both resonators with two separate electronic channels.[5] The proximity of the sample and reference sensors makes the reference particularly reliable. For instance, thermal equilibration between the reference and the sample is fast. Some additional difficulties may, however, arise because the two electrodes have to be coated with different materials. In special cases, temperature and pressure may have a different influence on the two coatings and thereby indirectly affect the sensor's specificity.

Interesting and potentially useful features appear if a somewhat narrower spacing between the electrodes is employed, resulting in a weak lateral coupling between the two resonators. In the following, we explore the behavior of such a system and demonstrate the application for sensoric purposes.

EXPERIMENTAL SECTION

The experiments were performed on 5-MHz AT-cut quartz blanks (MaxTek, Torrance, CA) with a diameter of 1 in. Both surfaces were flat and optically polished. Gold electrodes with a thickness of 60−100 nm were evaporated onto the quartz blanks through a mask. There are two electrode pairs forming two electromechanical resonators (Figure 1). The electrodes are keyhole-shaped in order to confine the mechanical waves via energy trapping.[6,7] The amplitude of oscillation decays exponen-

* Corresponding author: (phone) 49-6131-379 163; (fax) 49-6131-379 360; (e-mail) johannsmann@mpip-mainz.mpg.de.

(1) Lu, C., Czanderna, A. W., Eds. *Applications of Piezoelectric Quartz Crystal Microbalances*; Elsevier: Amsterdam, 1984.
(2) Schumacher, R. *Angew. Chem., Int. Ed. Engl.* **1990**, *29*, 329.
(3) Johannsmann, D. *Macromol. Chem. Phys.* **1999**, *200*, 501.
(4) Rickert, J.; Brecht, A.; Göpel, W. *Biosens. Bioelectron.* **1997**, *12*, 567.
(5) Srikhirin, T.; Laschitsch, A.; Neher, D.; Johannsmann, D. *Appl. Phys. Lett.* **2000**, *77*, 963.
(6) Bottom, V. E. *Introduction to Quartz Crystal Unit Design*; Van Nostrand Reinhold: New York, 1982.

10.1021/ac000692+ CCC: $20.00

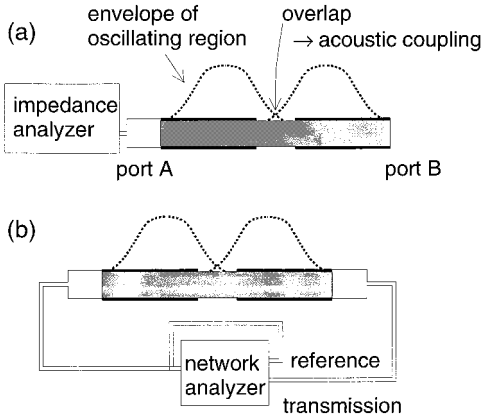

Figure 2. Configurations of measurement. (a) Impedance mode: One port is connected to an impedance analyzer. (b) Transmission mode: The transmission through the coupled system ("S_{21}") is measured with a network analyzer.

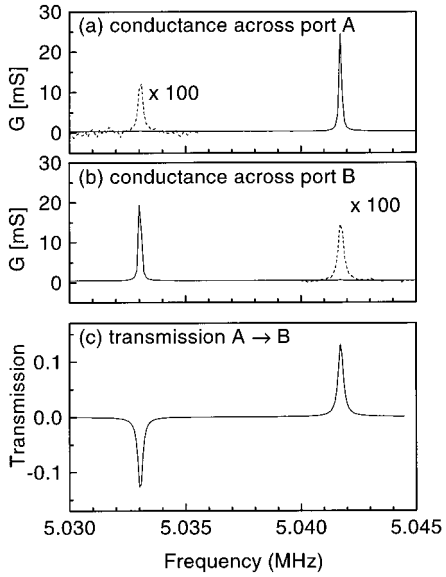

Figure 3. Typical data for a weakly coupled system under conditions where the individual resonators are detuned. The gold electrodes were 100 nm thick; a 102-nm-thick dextran film was deposited on one electrode. The lateral electrode distance was $d = 3$ mm, and the electrode radius was 3 mm. In the impedance mode (Figure 2a) the conductance spectrum $G(f)$ is dominated by the resonator directly connected to the impedance analyzer. The other resonance is hardly detectable. In the transmission mode (Figure 2b), both resonances appear equally strong.

tially with increasing distance from the electrode. If the oscillating regions of the two resonators slightly overlap, coupling results. It is expected that the coupling decreases with increasing distance d between the electrode pairs. The distance d varied between 1.8 and 4.5 mm. An effectively decoupled situation also is obtained if the resonators are sufficiently detuned, for instance, by making one electrode much thicker than the other.

The resonance parameters were passively measured with an HP 4195A network analyzer. We used the impedance mode to determine the conductance $G(f)$ across the individual electrode pairs (Figure 2a) and the network mode to determine the transmission (Figure 2b) through the coupled system ("S_{21} parameter"[8]).

IMPEDANCE AND TRANSMISSION SPECTRA

(a) Detuned Resonators. We first discuss the case where the resonance frequencies of the two resonators are much different. This is realized in experiment by choosing different electrode thicknesses. In Figure 3 a and b we show the conductance $G(f)$ across the two ports as a function of frequency f. The electrode distance in this particular case was $d = 3$ mm. The gold electrodes were ~100 nm thick. One electrode was covered with a 102-nm dextran film. The conductance spectra in Figure 3a and b are dominated by a single peak. Upon close inspection, however, one finds the second resonance as well, albeit at a much lower amplitude. Both resonances can be measured simultaneously in the "network" mode (Figure 3c). Although the transmission is small, the resonances are determined with good accuracy because the measurement is free of background. The resonance frequencies determined in the different modes agree within a relative accuracy of $\Delta f/f \sim 10^{-6}$. The transmission has an opposite sign for the two resonances because of the parallel and antiparallel motion of the individual resonators on the lower and the higher resonances, respectively. The parallel motion results in a negative amplitude of transmission because on resonance there is a phase shift of 90° between the exciting electrical signal and the mechanical response. The same phase shift occurs between the mechanical motion and the emitted secondary wave, adding up to a total phase shift of 180° between the primary and the secondary electric waves. For the resonance with the higher frequency, this phase shift is compensated by the antiparallel motion.

(b) Symmetrical Configuration. Even if the gap between the resonators is small, the resonance frequencies of the individual resonators are largely unperturbed by the second resonator as long as the two resonators are sufficiently detuned. If, on the other hand, the resonance frequencies are close to each other, one finds the familiar splitting into parallel and antiparallel resonances.[9] When tuning the frequency of one resonator across the resonance frequency of the second resonator, the resonance frequencies of the coupled system never cross.

This behavior is easily demonstrated in the configuration shown in the top panel in Figure 4. The measurement occurs across port A, which is connected to the impedance analyzer. Port B is short-circuited across a variable shunt resistor R_v. The resistor affects the stiffness of the quartz plate via piezoelectric stiffening. Because the "open" and the "short-circuited" elastic constants of piezoelectric materials are different,[10] the resonance frequency can be tuned over a range of $\Delta f/f \sim 10^{-4}$ by electrical means. This is enough to demonstrate the level splitting. The shunt resistor has the same effect as a mass loading. It is unrelated to the resistance on the peak of the resonance, which is frequently used to assess viscous dissipation.

(7) In hindsight, it would have been advantageous to displace the flags of the electrodes relative to each other. Flags on top of each other may have induced distortions of the mode shapes.

(8) Meinke, H.; Gundlach, F. W. *Taschenbuch der Hochfrequenztechnik*, 5th ed.; Springer-Verlag: Heidelberg, 1992; pp C3−C17.

(9) Landau, L. D.; Lifschitz, E. M. *Lehrbuch der Theoretischen Physik, Band 1, Mechanik*, 13th ed.; Akademie-Verlag: Berlin, 1990; pp 79−89.

(10) Thurston, R. N. In *Mechanics of Solids*; Truesdell, C., Ed.; Springer-Verlag: Heidelberg, 1984; Vol. 4, Chapter 36, p 257,

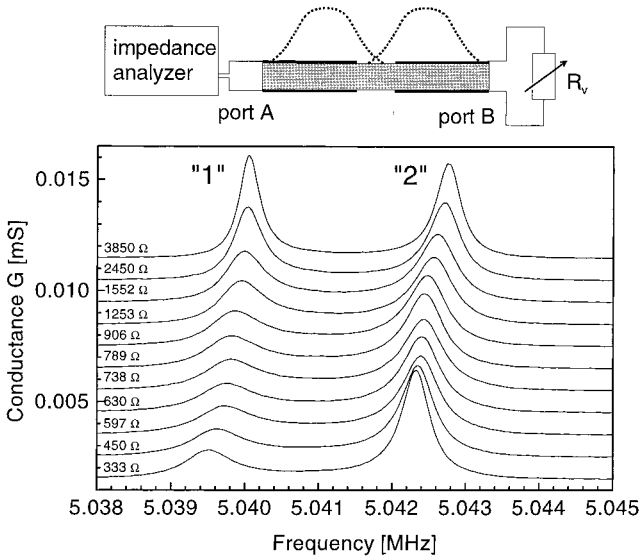

Figure 4. "Level splitting", well known from coupled pendulums, for a weakly coupled symmetrical system ($f_A \approx f_B$). The lateral distance between the 100-nm gold electrodes was d = 2.5 mm. As the frequency f_B is tuned across f_A (which remains fixed) by means of the variable shunt resistor R_v, the system crosses the symmetrical situation. The resonance frequencies of the coupled system, however, never cross. In the symmetrical situation, the two peaks correspond to a parallel and an antiparallel motion of the two resonators. The spectra have been vertically displaced for clarity.

The top data trace in Figure 4 corresponds to a slightly asymmetric configuration ($f_B > f_A$). The resonance frequency of the (hypothetical) isolated resonator B, f_B, is higher than the frequency of the (hypothetical) isolated resonator A, f_A. However, both resonances are so close that the eigenmodes (termed "1" and "2") of the coupled system are not given by localized movements but rather by a cooperative movement of both resonators. The lower data traces display conductance spectra as the shunt resistor, R_v, is varied. The symmetric situation ($f_B = f_A$) is reached for a shunt resistance of $R_v \sim 2000\ \Omega$. In the perfectly symmetrical situation, both peaks are equally high; that is, both resonators oscillate with an equal amplitude. The lower and the higher frequencies, f_1 and f_2, correspond to a parallel and an antiparallel motion, respectively. At very low shunt resistance, the asymmetry has been reversed. For the detuned situation (top and bottom traces in Figure 4), the amplitudes are distributed asymmetrically. The resonance that is preferentially located on resonator A (connected to the impedance analyzer) has the larger electrical amplitude.

In Figure 5, we show the center frequencies of the resonances as a function of the shunt resistance R_v. For comparison with theory, one would want to plot the resonance parameters of the composite resonator against the frequency of the individual resonator B, f_B. However, we have no direct way of inferring the frequency f_B from the resistance R_v. We therefore plot the resonance parameters versus the arithmetic average of the two resonances $1/2\ (f_1 + f_2)$ in Figure 6. With the equivalent circuit from Figure 7 (discussed in detail in the Equivalent Circuit section and in the Supporting Information), one finds that this frequency is close to $^1/_2\ (f_B + f_A)$ (f_A = constant) and, therefore, is a good measure of the frequency of the tuned resonator. Qualitatively,

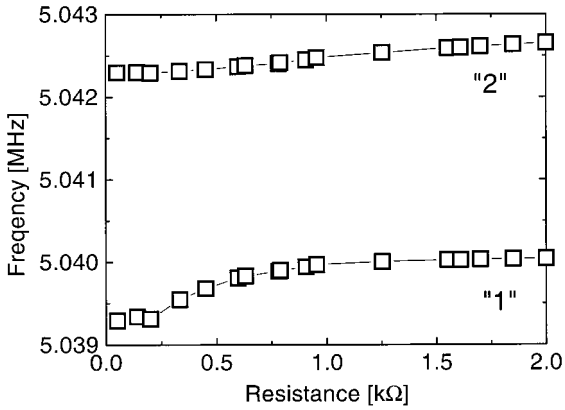

Figure 5. Resonance frequencies f_1 and f_2 as a function of the shunt resistance R_v.

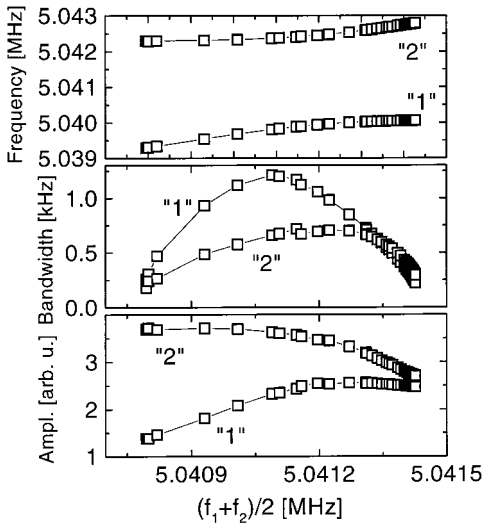

Figure 6. Frequency, bandwidth, and amplitude of resonances 1 and 2 from Figure 4 as a function of the arithmetic mean of the resonance frequencies $^1/_2(f_1 + f_2)$. The coupled resonator model (see Supporting Information) predicts that $^1/_2(f_1 + f_2) \approx {}^1/_2(f_A + f_B)$. Since f_A is constant, the arithmetic mean is a good measure of f_B.

the behavior agrees well with the phenomenology known from coupled pendulums. It can be summarized as follows:

(a) The resonance frequencies of the composite resonator never cross. In the symmetrical situation ($f_A \approx f_B$), there is a splitting by a frequency $f_c = f_2 - f_1$ which is a measure of the coupling strength. Both resonators are excited on both resonance frequencies. The lower and the higher resonance frequencies correspond to a parallel and an antiparallel motion, respectively.

(b) The bandwidth of both resonators goes through a maximum close to the symmetrical situation. Here coupling is strong. Apparently, coupling is accompanied by dissipation. This can be rationalized by assuming that the modes with equal amplitudes on both resonators have a rather complicated displacement pattern. The increased complexity presumably entails flexure contributions which radiate longitudinal sound and therefore dissipate energy.

(c) The amplitude of oscillation varies. As f_B decreases, the amplitude of resonance "1" increases, while the amplitude of resonance "2" decreases. This reflects the relative contributions of resonator A to the modes "1" and "2".

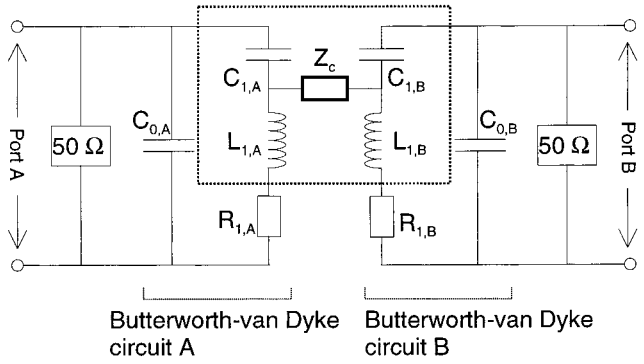

Figure 7. Equivalent circuit representing the simplest way to couple two Butterworth−van Dyke resonators. Coupling occurs across a coupling impedance Z_c. The subcircuit in dashed lines is the electrical analog of coupled pendulums. Its resonance frequencies can be analytically derived (see Supporting Information).

EQUIVALENT CIRCUIT

The qualitative behavior of the composite resonator agrees with what one expects for the "coupled pendulums" picture. When modeling the composite resonator with an equivalent circuit, we therefore draw on this analogy. One usually describes the electromechanical properties of an isolated thickness-shear resonator close to resonance by the Butterworth−van Dyke circuit.[11] The acoustic branch of the resonator is given by a motional inductance L_1, a motional capacitance C_1, and a motional resistance R_1. Its resonance parameters may be rearranged to the variables $\omega_0 = 2\pi f_0 = (L_1C_1)^{-1/2}$ (resonance frequency), $Z_0 = (L_1/C_1)^{1/2}$ (resonance impedance), and $Q = 2\pi Z_0/R_1$ (quality factor). C_0 represents the electrical capacity of the electrodes. In Figure 7, we show the simplest way of coupling two such Butterworth−van Dyke circuits. Coupling is introduced by a complex coupling resistance Z_c. In an electrical representation, one would probably choose Z_c to be a coupling capacitor. Because the node providing coupling is placed in the middle of the series resonance circuits, the flow through Z_c is much enhanced when either the emitter or the receiver is on resonance.

Applying Kirchhoff's laws to the entire circuit in Figure 7, the conductance across port A is straightforwardly calculated. Figure 8 shows the result of such a calculation as a contour plot. The conductance spectra are vertical cuts through this plot. The two bands correspond to the resonance peaks. Considering only the central part of the circuit (dotted lines in Figure 7), the resonance frequencies of modes "1" and "2" can be approximated analytically, as well. The rather technical calculation is available as Supporting Information. It yields the resonance frequencies of modes 1 and 2 as

$$f_{1,2}^2 = \frac{1}{2}\frac{\beta \pm \sqrt{\beta^2 - 4f_A^3 f_B^3 \alpha}}{\alpha}$$

$$\alpha = f_A f_B + f_c(f_A + f_B)$$

$$\beta = f_A f_B((f_A^2 + f_B^2) + f_c(f_A + f_B)) \qquad (1)$$

where f_A and f_B are the resonance frequencies of the individual resonators. The frequency f_c quantifies the coupling strength. It is defined as $f_c = (f_A f_B/f)\ (L_1/C_1)^{1/2}/\ Z_c$. In the symmetrical situation ($f_A = f_B$), the parallel and the antiparallel resonances differ in frequency by f_c. The thick lines in Figure 8 are the resonance frequencies of the coupled system according to eq 1. They coincide well with the maximums of conductance.

Figure 9 shows calculations where we have tried to reproduce the data from Figure 6 with the equivalent circuit. The frequencies were calculated with eq 1. The calculation of the bandwidths and the amplitudes is available as Supporting Information. The general behavior is reproduced. When the frequency of resonator B is being tuned, the frequencies, bandwidths, and amplitudes of the

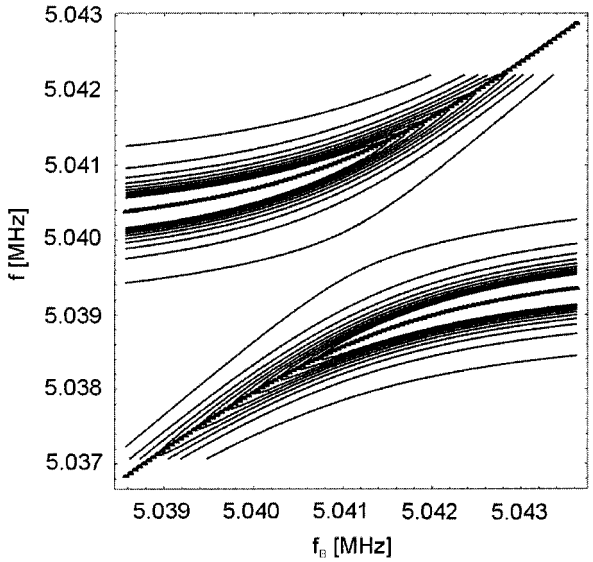

Figure 8. Contour plot of the conductance $G(f,f_B)$ across port A for a variable frequency f_B of resonator B calculated for the equivalent circuit from Figure 7. For the calculation, port B was short-circuited across a 50-Ω resistor. The thick lines are the resonance frequencies as calculated with eq 1.

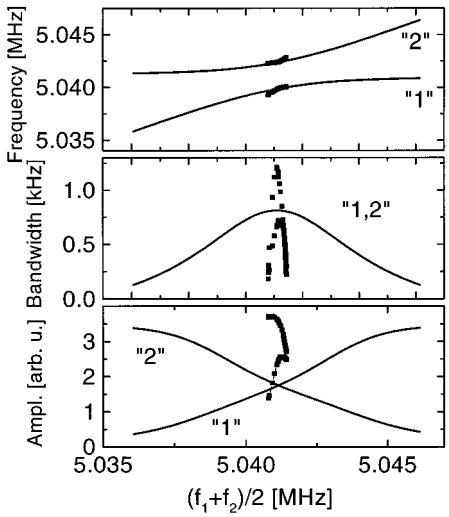

Figure 9. Frequency, bandwidth, and amplitude of resonances 1 and 2 as a function of the arithmetic mean of the resonance frequencies $^1/_2(f_1 + f_2)$ calculated with the simple coupled resonator model. The fit parameters are $f_A = 5.041$ MHz and $f_c = 2.5 \times (1 + 0.8i)$ kHz. The experimental data (dots) from Figure 6 are only qualitatively reproduced. The range of frequencies, where coupling occurs, is narrower in experiment.

(11) Rosenbaum, J. F. *Bulk Acoustic Wave Theory and Devices*; Artech House: Boston, London, 1988; pp 167−199.

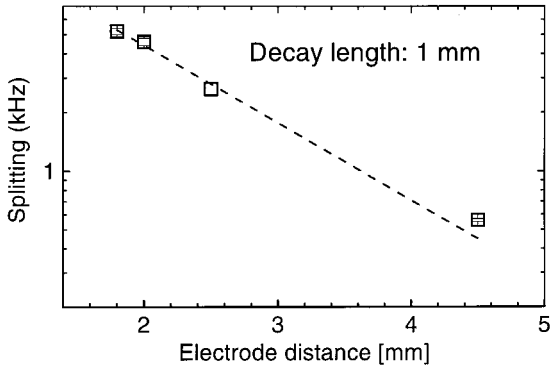

Figure 10. Coupling parameter f_c as a function of electrode distance for uncoated quartzes on a logarithmic scale. From the fit with a single exponential (dotted line), one infers that the evanescent tail of the oscillating region outside the electrodes has a length of ~1 mm.

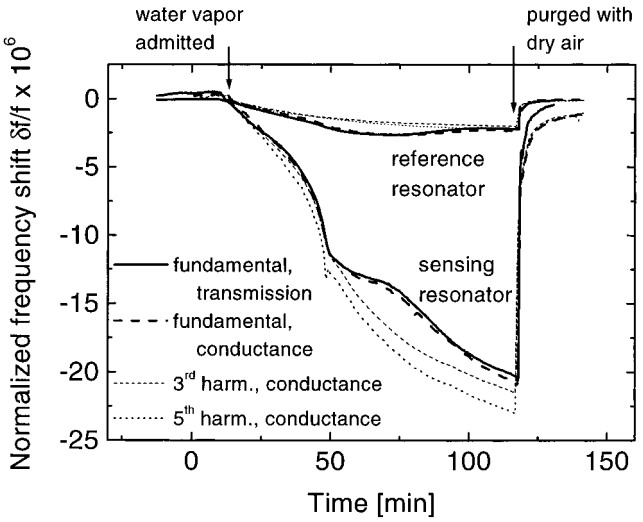

Figure 11. Resonance frequencies of a composite resonator (3-mm lateral electrode distance, 100-nm-thick gold electrodes), where one electrode has been coated with a water-swellable dextran film (thickness 102 nm). When water vapor is introduced into the sample compartment, the frequency of the sensing resonator decreases. The reference resonator responds to the increased humidity and effects of temperature. It can therefore be used to subtract these environmental disturbances.

composite resonator change as in the experiment (Figure 6). More quantitatively, there are significant differences between the experimental data and the model, as well. This mostly concerns the width of the region where coupling is strong. By this region we mean frequencies where the modes are distributed over both electrodes. The simple coupled resonator model predicts that this range is about as wide as the coupling frequency f_c, the latter being fixed by the splitting between the parallel and the antiparallel modes. Both the bandwidths and the amplitudes indicate that in the experiment the regime of coupling is much narrower than $\pm f_c$. Evidently, the simple model of coupling through a single complex resistance does not yield quantitative agreement with the data. The limitations of such a simple model do not come as a surprise. Modeling the 3D mode pattern of a quartz crystal with discrete mechanical elements such as springs and dashpots is quite a crude approximation. A further indication of such shortcomings is the fact that we could not find convincing examples of coupling on any of the overtones. On the overtones, the displacement pattern becomes even more complicated.

Varying the electrode spacing mainly affects the coupling strength, which in turn determines the frequency splitting between the peaks and their amplitudes (Figures 4−6). The splitting in the symmetrical situation provides a convenient measure of the coupling strength. For the system shown in Figure 4 (d = 2.5 mm), one has $(f_1 - f_2)/f \sim 4 \times 10^{-5}$. Figure 10 shows the frequency splitting as a function of electrode distance (electrode thickness: 100 nm, no additional films on the electrodes). As expected, the splitting decreases with increasing electrode distance. The dotted line is the best fit to an exponential. The slope corresponds to a decay length of the oscillating regions outside the electrodes of 1 mm.

There is a remarkable similarity between the lateral coupling of two resonators and the coupling between a quartz resonator and soft film of thickness $\lambda/4$ on top of one electrode (λ the wavelength of shear sound). The latter situation is usually termed "film resonance".[12,13] The coupling in this case is weak because of the large impedance mismatch between the quartz and the film. The shear waves are strongly reflected at the quartz−film interface. As has been pointed out recently, the film resonance is also characterized by a splitting.[14]

SENSOR APPLICATION

Finally, we show that the coupled system can be used for sensor applications. If the two resonators have coatings that respond differently to the presence of a certain analyte, differential measurements of affinity become possible. In the experiments reported here, the analyte is water vapor, which swells a dextran film deposited on one of the two resonators. The second resonator (exposing a hydrophobic gold surface) serves as a reference. It is influenced by the same environmental factors as the sensing unit but does not specifically respond to the presence of the analyte.

A water-swellable dextran film was spin-cast onto one side of the quartz plate from aqueous solution at a speed of 1500 rpm. The molecular weight was M_w = 200 000−300 000 according to the supplier. Prior to film deposition, the gold electrodes were exposed to an argon−oxygen plasma for 5 min at 280 W in order to make the gold surface hydrophilic. The thickness d_{film} was adjusted via the solute concentration to a value of d_{film} = 102 nm. The dextran film was wiped off from the reference electrode, such that only the sensing electrode remained covered.

Figure 11 shows the evolution of various overtones as water vapor is admitted to the sample chamber. The thick straight and the thick dashed lines show the frequencies of the fundamental mode measured in the network mode and the impedance mode, respectively. All thin dashed lines represent the third and the fifth harmonics measured in the impedance mode. The data in Figure 11 are a superposition of two different experiments performed under the same conditions. The solid line in boldface corresponds to an experiment in which the sensing and the reference frequencies have been determined at the same time in the

(12) Martin, S. J.; Frye, G. C. *Ultrason. Symp.* **1991**, *393*.

(13) Johannsmann, D.; Mathauer, K.; Wegner, G.; Knoll, W. *Phys. Rev. B* **1992**, *46*, 7808.

(14) Martin, S. J.; Bandey, H. L.; Cernosek, R. W.; Hillman, A. R.; Brown, M. J. *Anal. Chem.* **2000**, *72*, 141.

transmission mode. In all other cases, the data were acquired by impedance measurements, where the sensing and the reference resonators were connected to the two input channels of the impedance analyzer.

Clearly, both the frequency of the probe and the frequency of the reference shift upon admission of water vapor. The frequency shifts of the fundamental are very similar in the transmission and in the conductance modes, the slight variability probably being caused by differences in the evolution of water vapor pressure in the two experiments. For the third and the fifth harmonics, the resonances are so weakly coupled that a measurement in the transmission mode was impossible. These resonances allow for an estimation of the influence of coupling onto the reference frequency. In principle, the frequency of the reference resonator may shift not only because of the environmental disturbances but also because of the coupling to the sensing resonator. When measuring in the transmission mode, one has to find a balance between a strong-enough coupling permitting some transmission, on one hand, and a weak-enough coupling minimizing the influence of coupling onto the frequency of the reference resonator, on the other hand. Detuning the two resonators also works in favor of small coupling. The comparison with the evolution of the frequencies of the (decoupled) overtones proves that sufficient decoupling has been achieved. The overtone frequencies of the reference resonator behave similarly to the fundamental. Evidently, the shift of the reference frequency is governed by effects of temperature and viscosity of the air and may be subtracted from the frequency of the sensing resonator in order to more accurately determine the amount of water accumulated in the dextran film.

Coupling can also provide some insight when multielement arrays on a single quartz wafer are designed.[15] In case coupling is to be avoided, this can be checked in a transmission experiment. Possibly, some compromise has to be found in order to increase the density of sensing elements. One would correct for the concurrent cross-talk between the different elements in the analysis. Precise calibration of the coupling will be necessary. Note that coupling might even be beneficial for read-out purposes because in the transmission mode two channels can be read out with a single electronic channel. One may even read out a resonator that is not electrically connected via its mechanical coupling to a neighboring element (Figure 3a and b). In this way, electrical leads are eliminated, which may save space on the wafer.

(15) Abe, T.; Esashi, M. *Sens. Actuators, A* **2000**, *82*, 139.

CONCLUSIONS

By placing two pairs of resonators onto one quartz blank one can generate a system of weakly coupled resonators. The coupling depends on the distance between the electrodes, the thickness of the electrodes, and the detuning. In symmetrical situations, the coupled modes are given by a parallel and an antiparallel oscillation of both resonators. An equivalent circuit based on the electromechanical analogy with coupled pendulums is proposed. The circuit qualitatively reproduces the experiments. This geometry is attractive for sensor applications because the two resonators can act as a probe and a reference in close proximity. Being exposed to the same environment they can be used for differential measurements of adsorption. The effects of temperature and humidity can be eliminated.

ACKNOWLEDGMENT

We thank Ralf Lucklum, Alfons Blum, and Alexander Laschitsch for helpful discussions.

SUPPORTING INFORMATION AVAILABLE

Derivation of eq 1. This material is available free of charge via the Internet at http://pubs.acs.org.

Received for review June 15, 2000. Accepted December 12, 2000.

AC000692+